Applied Thermal Engineering 179 (2020) 115671

Contents lists available at ScienceDirect

Applied Thermal Engineering

journal homepage: www.elsevier.com/locate/apthermeng

Modelling and off-design performance optimisation of a trilateral flash cycle system using two-phase twin-screw expanders with variable built-in volume ratio

Giuseppe Bianchi[a,*], Matteo Marchionni[a], Jeremy Miller[b], Savvas A. Tassou[a]

[a] Brunel University London, Institute of Energy Futures, Centre for Sustainable Energy Use in Food Chains, Uxbridge UB8 3PH, United Kingdom
[b] Spirax Sarco Engineering PLC, Cheltenham GL51 9NQ, United Kingdom

HIGHLIGHTS

- Sliding valve in the expander casing used to vary the built-in volume ratio (BIVR)
- Lower BIVRs improve volumetric efficiency but worsen specific indicated power.
- Expander BIVR and revolution speed affect most the heat to power conversion.
- Control variables optimised to boost nominal performance from 81 kW to 103 kW.

GRAPHICAL ABSTRACT

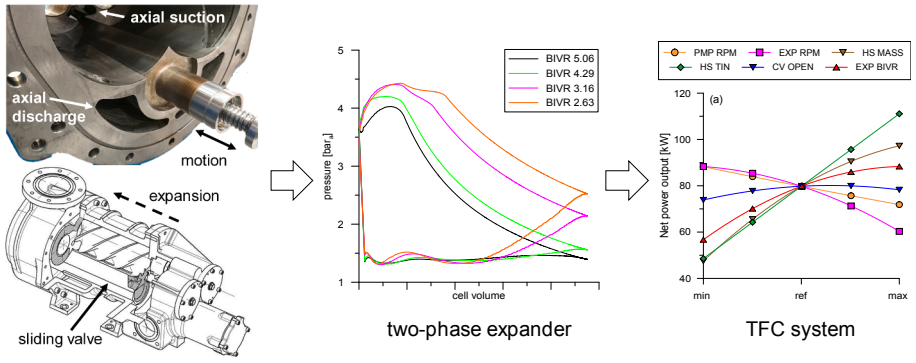

ARTICLE INFO

Keywords:
Trilateral flash cycle
Twin-screw expander
Two-phase expander
Low-grade waste heat recovery
Built-in volume ratio

ABSTRACT

This research work presents a numerical chamber model of a two-phase twin-screw expander and its further integration in a one-dimensional model of a Trilateral Flash Cycle (TFC) system for low-grade heat to power conversion applications. The novel feature of the expander is the capability of changing the built-in volume ratio (BIVR) of the machine through a sliding valve in the casing that opens an additional suction port. Lowering the BIVR from 5.06 to 2.63 results in an improvement of the volumetric efficiency from 53% to 77% but also in a reduction of the specific indicated power from 4.77 kJ/kg to 3.56 kJ/kg. Parametric analysis on several degrees of freedom of the full TFC system concluded that expander speed and BIVR are the variables that mostly impact the net power output of the unit. An optimisation study enabled the net power output of the TFC system, at design point, to increase from 81 kW to 103 kW.

1. Introduction

Low-grade waste heat to power conversion has recently attracted increased attention by the academic and industrial communities. The potential for thermal energy recovery and conversion to electricity from waste heat sources at temperatures below 100 °C has been estimated at 468 TWh on a European scale [1] and 43.2 PWh worldwide [2]. According to the aforementioned studies, the most promising sectors for harvesting this potential are the chemical and petrochemical, the non-metallic minerals as well as the food and tobacco industries.

* Corresponding author.
E-mail address: giuseppe.bianchi@brunel.ac.uk (G. Bianchi).

https://doi.org/10.1016/j.applthermaleng.2020.115671
Received 12 November 2019; Received in revised form 22 May 2020; Accepted 28 June 2020
Available online 03 July 2020

Nomenclature

e	specific total internal energy [J kg^{-1}]
c_p	specific heat at constant pressure [J kg^{-1} K^{-1}]
h	specific enthalpy [J kg^{-1}]
m	mass [kg]
$\dot{m}$	mass flow rate [kg s^{-1}]
p	pressure [Pa]
r	specific internal energy [J kg^{-1}]
t	time [s]
u	velocity [m/s]
x	quality
A	area [m^2]
B	total number of boundaries
H	heat transfer coefficient [W m^{-2} K^{-1}]
P_{ind}	indicated power [W]
R	equivalent gas constant [J kg^{-1} K^{-1}]
T	temperature [K]
V	volume [m^3]
Z	number of rotor lobes
γ	ratio of specific heats
η	efficiency
ρ	density [kg m^{-3}]
θ	valve lift
φ	control valve area ratio
ω	revolution speed [RPM]
01	total upstream conditions
2	static downstream conditions
is	isentropic
hot	heat source
leak	leakage
s	heat transfer surface
suc	suction
vol	volumetric

Among the available technologies, heat to power conversion systems are characterised by higher flexibility than heat exchanger networks for recovery and internal reuse of the energy and for over the fence export. Bottoming thermodynamic cycles, and particularly Organic Rankine Cycles (ORC), are a mature technology for waste heat to power conversion especially at medium heat source temperature levels in the range 150–300 °C and at power sizes in the order of megawatts [3]. For low-grade heat recovery applications, the academic literature proposes the trilateral flash cycle as a promising candidate for heat to power conversion [4].

The TFC differs from the ORC in the absence of phase change during the heat addition and expansion in the two-phase region of the organic working fluid. In [5], a TFC using water and four ORC configurations were compared considering an expander isentropic efficiency of 85%. The findings revealed 14–29% higher values of exergetic efficiency in the case of TFC depending on the inlet temperatures of heat source and sink. Moreover, the volume flow rate at the expander outlet was significantly higher in the TFC system, from 2.8 to 70.0 times greater than the ORC in the same operating conditions. Therefore, it was suggested the utilization of fluids with higher vapour pressures such as cyclopentane and butane. In a later study, based on the same conditions described in [5], a comparison was carried out between TFC operating with organic fluids and water, an ORC and a Clausius-Rankine cycle. The TFC with water outperformed all the other cycles in terms of exergetic efficiency [6].

Two-phase expansion technologies are commercially available for some niche applications. In the context of mechanical power generation from geothermal fluids, impulse steam turbines are the state of art at megawatt scale [7]. In addition to that, a 1 kW two-phase reaction turbine, whose concept was patented by Fabris [8], has been recently analysed and optimised through multi-phase Computational Fluid Dynamics (CFD) using the Thermal Phase-Change model [9]. In Liquefied Natural Gas (LNG) applications, a commercial radial turbine [10] resulted in an empirical isentropic efficiency up to 85% [11] with a power size in the order of tens megawatts.

To seize the opportunity provided by distributed low-grade waste heat sources, an ideal electrical power size for TFC systems ranges around 100 kW. In fact, this allows transportability of the power recovery units, use of off-the-shelf equipment, low footprint and installation complexity, and a still adequate business case [12]. At this scale, positive displacement machines are more preferable than the dynamic ones given the high-pressure ratios and the relatively small mass flow rates. Nonetheless, research is also ongoing to develop TFC impulse turbines. In particular, an experimental study on the converging–diverging nozzle of a TFC impulse turbine showed a progressive increase in the nozzle efficiency by a rise in the inlet temperature of iso-pentane up to 45% at 68.3 °C [13]. On the other hand, an Euler impulse turbine operating with R245fa resulted in an experimental power recovery up to 7 kW. The study further highlighted a number of advantages of TFC compared to ORC, such as up to 80% additional power output at the same operation conditions as well as simplified control of the heat to power block [14].

Unlike those positive displacement technologies that experience a limitation in the revolution speed to minimise the friction losses occurring between stationary and moving parts, twin-screw expanders can operate at high speeds, up to 6000 RPM. This feature results in the capability of processing large quantities of flow and reduced investment costs. As such, even though some studies on reciprocating TFC expanders are also available [15], most of the published literature focuses on the twin-screw technology.

Twin-screw machines have been thoroughly investigated through numerical and experimental approaches when used as air or refrigeration compressors and as ORC expanders [16]. Among them, some commercial solutions for two-phase ORC expanders have been also developed [17,18], while a recent analysis concluded that for heat source temperatures ranging between 80 °C and 200 °C, the optimal critical temperature of the working fluids ranges between 125 °C and 175 °C, (e.g. R245ca, iso-pentane and n-butane) [19]. Nonetheless, to the best of the authors' knowledge, the availability of literature on two-phase twin-screw expanders for TFC applications is not sufficiently thorough to provide a deep understanding of the underpinning physics of the flash expansion in these machines.

The first research outputs on twin-screw expanders for TFC applications are from the research group at City University London. In [20], a 10 year study on TFC and twin-screw expanders is presented. Extensive numerical and experimental activities were carried out with the then available working fluids. Results reported an output power in the order of 25 kW and isentropic efficiency close to 70%. The authors also highlighted the issue of pre-expansion during the initial filling working chambers. The chamber model developed, assuming homogeneous two-phase flow, also showed a good agreement with the experimental results. In [21], the geometrical optimization of a twin-screw machine for the expansion of wet steam is presented. With reference to a model which calculated the two-phase fluid properties as the average of the single phase ones weighted on the quality, the numerical work proposed a multi-variable geometric optimization to maximise the output power. The optimized geometry was tested at different expansion ratios and achieved isentropic efficiency greater than 70% at nominal conditions.

In [22], a thermodynamic modelling for TFC twin-screw expanders is presented. The modelling approach considers the filling process as if the working chambers are filled with a hot liquid over an injector

nozzle rather than an inlet area to improve flash vaporization of the fluid. The leakage calculation is instead handled with a homogeneous mixture approach. As concerns the energy equation, a thermodynamic equilibrium is considered. This assumes that sufficient heat transfer exists between the phases to reach a stable state within a time step. The simulations showed good agreement with measurements performed on a steam expander, even though deviations on the power output and indicator diagram were noticed especially at low revolution speeds.

In [23], extensive experimental investigations are carried out on a water injected twin-screw expander, including indicating pressure measurements. The experiments showed a better volumetric efficiency at lower revolution speeds and an almost constant mechanical efficiency when the quality ranged between 0.97 and 0.99. This result agrees with the simulations performed in [24] in which it is concluded that at high steam qualities, the specific flow consumption (i.e. ratio between power recovered and steam used) is optimal.

In [25], the impact of different rotor-tip clearance heights was investigated concluding that greater rotor-tip gaps, albeit providing a greater mechanical efficiency, result in lower power recovery performance due to worse indicated and isentropic efficiency.

In [26], a correlation between isentropic efficiency and inlet quality is proposed based on data from previous experimental works on two-phase twin-screw expanders, [20,27,28]. The correlation indicates that differences in adiabatic efficiency tend to level out with reducing vapour fraction. Designs with poor peak efficiency tend to improve at low vapour fraction conditions while designs with high peak efficiency become less efficient at lower vapour fractions.

The effects of surface condensation in steam-driven twin-screw expanders were recently assessed through a chamber model simulation coupled with a thermal analysis for the heat transfer between fluid and metallic surfaces. The study concluded that, due to the short time scales and the periodicity of the expansion, the condensation process is best described by models for dropwise condensation. Moreover, the research asserted that condensate is trapped in the working chamber at the end of the filling period, thus increasing the mass flow rate of the machine but with no effects on the power output [29].

All the research works agree on the complexity of the phenomena involved in a flashing expansion in screw machines. Hence, some researchers began to investigate the fundamentals in more simplified machines, namely piston geometries [30]. A two-phase piston expander was also experimentally and numerically investigated in [31]. From the experimental investigations, it was identified that the mixing of the liquid due to boiling bubbles was found to have a strong impact on pressure change during adiabatic expansion. Hence, two-phase adiabatic vaporization in a cylinder is considered to be mainly dominated by the heat transfer between the bulk liquid and the gas–liquid interface. These operating conditions, however, are not fully representative of the reality in twin-screw machines since the phase change process takes place while the fluid in the control volume rotates and simultaneously mixes with other flows.

In this context, the current research proposes to address the knowledge gap related to the expander operation as well as the interaction effects between the different components of a TFC system in terms of sensitivity and impact on recovery performance also at off-design conditions. The novelty of the research methodology employed in this work lies in the scalability of the results for optimization and control studies. Another element of novelty compared to the state of the art is the numerical investigation of the effects that a variation of the expander built-in volume ratio has on the machine performance and the overall power recovery. This work also expands recently published work on Trilateral Rankine Cycles and partial-evaporating cycles, such as [32,33] and [34] respectively.

In Section 2, after introducing modelling methodology, the concept of variable built-in volume ratio (BIVR) presented. Section 3 instead focusses on the novel modelling features of the TFC heat to power unit presented in [12]. In Section 4, a first set of simulations on the standalone twin-screw machine is followed by the off-design performance assessment of the TFC unit. Maps reporting the optimal operating conditions for given temperatures and flow rates of the heat source are eventually presented and discussed.

2. Twin-screw expander modelling

2.1. Fundamentals

The twin-screw expander and the other components of the TFC system have been modelled in the commercial software platform GT-SUITE™ [35]. In this environment, positive displacement machines are modelled through lumped parameter formulations, also known as chamber models [36]. As concerns piping and heat exchangers, a one-dimensional formulation of the conservation equations solved with a staggered grid approach is instead considered. Dynamic machines such as the centrifugal pump of the TFC system are eventually modelled using a map-based approach [37].

The expander performance maps discussed in Section 3.1 were generated through the standalone expander model presented in [36] and adapted to include the variable built-in volume ratio capability. The cornerstone of this modelling approach, which applies to any positive displacement machine, is the energy equation expressed in terms of conservation of total internal energy, i.e. the sum of internal energy and kinetic energy ($e = r + u^2/2$). The energy Equation (1) states that, neglecting variations of potential energy, the rate of change of total internal energy in the expander chambers depends on their volume variation, the enthalpy fluxes through the boundaries (leakages, suction and discharge ports) and the heat transfer phenomena with casing and the rotors (neglected in the current case).

$$\frac{d(me)}{dt} = -p\frac{dV}{dt} + \sum_{i=1}^{B}\left(\dot{m}_i\left(e_i + \frac{p_i}{\rho_i}\right)\right) - HA_s\left(T_{fluid} - T_{wall}\right) \tag{1}$$

This lumped parameter formulation assumes no spatial variation of the fluid properties inside the expander chamber. The two-phase fluids are treated as equivalent gases whose thermophysical properties are calculated as the weighted average of the saturated liquid and vapour states based on quality. Eq. (2) reports an example for the ratio of specific heats.

$$\gamma = \gamma_{vap}x + \gamma_{liq}(1 - x) \tag{2}$$

Leakage flows as well as filling and emptying processes are treated as flow through an orifice whose equivalent diameter is an input of the calculation. In the case of subsonic flows, Eq. (3) applies.

$$\dot{m}_{leak} = A_{leak}\left(\rho_{01}\left(\frac{p_2}{p_{01}}\right)^{1/\gamma}\right)\sqrt{RT_{01}}\left(\frac{2\gamma}{\gamma - 1}\left(1 - \left(\frac{p_2}{p_{01}}\right)^{\frac{\gamma-1}{\gamma}}\right)\right)^{1/2} \tag{3}$$

In absence of friction losses, the expander power output equals to the indicated power Eq. (4).

$$P_{ind} = Z_{male}\frac{\omega}{60}\oint pdV \tag{4}$$

The volumetric efficiency is defined as the ratio between the mass flow rate resulting from the simulation and the theoretical value that can be calculated from the geometrical and operational characteristics of the machine according to Eq. (5).

$$\eta_{vol} = \frac{60\,\dot{m}}{\rho_{suc}V_{suc}Z_{male}\,\omega} \tag{5}$$

The isentropic efficiency is eventually calculated as the ratio of the real and the isentropic enthalpy drops across the expander, i.e. with inlet and outlet enthalpies measured at mid-length of the intake and exhaust ducts respectively, Eq. (6).

$$\eta_{is} = \frac{h_{01} - h_2}{h_{01} - h_{2,is}} \quad (6)$$

2.2. Variable built-in volume ratio

In positive displacement expanders, the fluid intake occurs through a narrow port which is designed to guide the high-pressure compressible flow through the expander cells. In TFC applications, this port has to provide suitable opening for a flow whose density can easily fluctuate if the system is not operating at design or steady state conditions (startup, transients, shutdown). From test experience, it has been identified that a large amount of liquid flowing through the suction port creates severe instability in the expander operation and significant noise and vibrations. The purpose of the sliding valve is therefore to mitigate these phenomena as well as change the built-in volume ratio (BIVR) of the machine to cater for different operating conditions.

The variation of the expander BIVR takes place through a sliding valve, i.e. a regulation screw that drives the linear motion of the bottom part of the casing. This approach essentially creates an additional suction port that, unlike the one on the high-pressure end wall of the expander, is radial and not axial. When the screw is completely tightened, the expander has a conventional layout with only the axial suction port. Otherwise, there is a cubic relationship between number of turns of the regulation screw and expander BIVR. The opening of the radial suction port requires an accurate modelling of the twin-screw expander geometry to be retrieved and, in the current study, it was provided by the manufacturer. The implementation of the sliding valve in the modelled twin-screw expander is reported in Fig. 1 while Fig. 2 shows the angular evolution of cell volume, discharge port area as well as radial and axial suction ports areas; the data reported span the available BIVR range (2.63–5.06) in four positions of the regulation screw.

The availability of the geometrical data of Fig. 2, together with the equivalent areas of the leakage paths, is essential for the expander modelling using the approach proposed in this paper. As such, should not these data be available, one should either liaise with the manufacturer or rely on geometrical pre-processors for twin-screw machines commercially available [38] or even measured from Computer-Aided Design software [39]. Additional information on the expander used as test case in the current work are reported in Table 1 [36].

Boundary conditions for the simulations were pressure and enthalpy at the inlet duct of the expander, pressure and quality at the outlet duct and revolution speed (Table 2). The variable combination used for the inlet boundary conditions allows single and multi-phase simulations. This is particularly relevant when the expander is integrated in the full TFC system model. Moreover, the quality boundary condition at the outlet of 0.4 applies only in the case of backflows, which is unlikely to happen in this application.

3. TFC system modelling

To assess the effect of the variable expander geometry on the system performance, a holistic model of a TFC-based heat to power conversion system has been also developed in GT-SUITE™. The model block diagram is shown in Fig. 3.

In the application here considered, the heat source and sink are both water streams while the working fluid is R245fa, whose thermophysical properties are retrieved through an interface with the NIST Refprop database [40]. Although it is being phased out, the reason for choosing this working fluid is to align the simulations with the ongoing experiments. Furthermore, in the TFC prototype being tested, a small quantity of POE oil was diluted in the R245fa since the expander bearings are lubricated through the working fluid. However, in the current study, the TFC was assumed to operate with pure working fluid since the actual quantity of oil through the expander and not accumulated in the heat exchangers is hardly quantifiable.

A control valve is eventually considered upstream of the expanders to regulate the fluid inlet conditions. In particular, if on one hand throttling the flow leads to a pressure loss, on the other one the higher quality of the working fluid may ensure a better expander operation. The novel modelling features developed in the current study deal with the expanders performance maps and the control valve.

3.1. Multi-dimensional expander performance maps

The performance maps of the expander are calculated using the model presented in the Section 2. In particular, the expander performance depends on the inlet quality of the working fluid, the manometric expansion ratio, the revolution speed and the BIVR [36]. Thus, all these parameters have been considered to predict the behaviour of the machine in the full TFC system model. To do that, the conventional templates available in the software cannot be used. Therefore, multi-dimensional look-up tables have been implemented. In these tables, the expander revolution speed, pressure ratio, inlet quality and the BIVR constitute the independent variables, while the mass flow rate and the isentropic efficiency of the machine are the dependent ones.

Each multi-dimensional map requires the combination of several two-dimensional maps having revolution speed and pressure ratio as independent variables. For instance, assuming three levels of variation for the inlet quality and three for the BIVR, the multi-dimensional map would require nine two-dimensional maps across which interpolations are performed.

The operating ranges of the independent variables were selected based on geometrical (BIVR) or functional characteristics or the machine (revolution speed) [36] as well as considerations resulting from the cycle analysis (cycle pressure ratio, fluid quality at the expander inlet) [12]. More specifically, the revolution speed was varied between 1500 RPM and 6000 RPM, the expansion ratio from 1.5 to 8.5, the refrigerant quality between 0.0 and 0.6, and the BIVR from 2.63 to

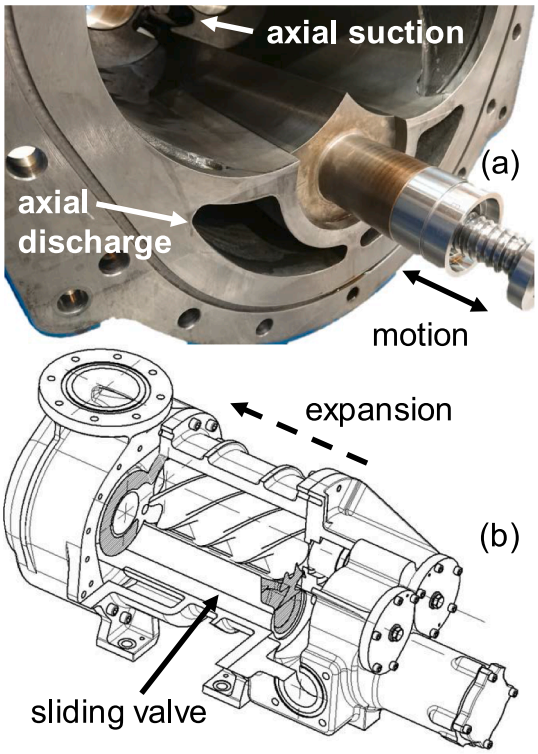

Fig. 1. Sliding valve implementation in the modelled twin-screw expander: (a) picture of the expander with the valve fully tightened, (b) 3D view of the machine having the sliding valve fully open (courtesy of Howden Compressors Ltd.)

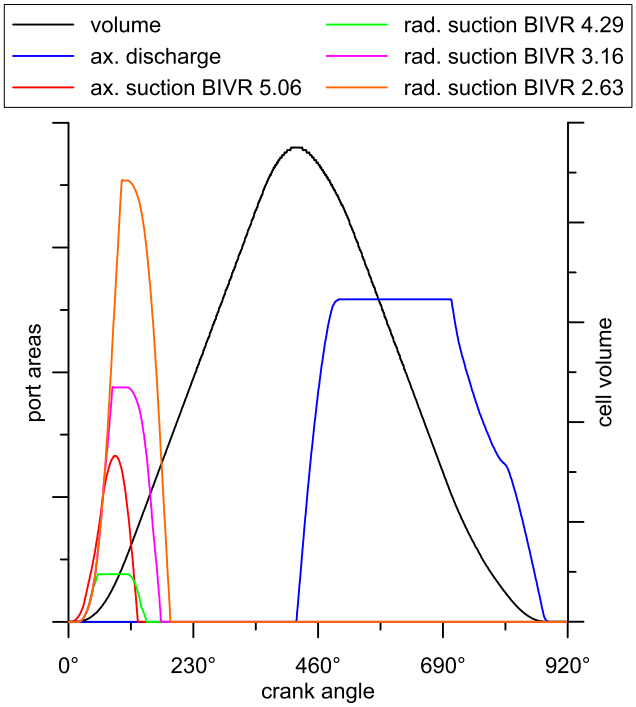

Fig. 2. Angular evolution of expander cell volume and ports areas in four positions of the sliding valve (courtesy of Howden Compressors Ltd.)

Table 1
Main geometrical and operating features of the modelled expander.

Rotor diameter	204 mm
Aspect ratio(L/D)	1.65
Built-in volume ratio	2.63–5.06
Male/female rotor lobes	4/6
Suction/discharge ports arrangement	axial/axial
Revolution speed range	1500–6000 RPM
Tip speed range	16–64 m/s
Weight	887 kg

Table 2
Simulation setup for Figs. 4 and 5.

Working fluid	R245fa
Revolution speed	3750 RPM
Inlet pressure	5.0 bar
Outlet pressure	1.3 bar
Outlet quality	0.4
Inlet enthalpy (quality = 0.1)	301 kJ/kg

5.06.

The multi-dimensional look up is carried out as follows: (1) the expander pressure ratio is calculated from the high and low cycle pressures which output from the heat exchangers sub-models; (2) the fluid quality at the expander inlet results from the energy balance at the heater; (3) the expander BIVR and revolution speed are given as boundary conditions; (4) mass flow rate and isentropic efficiency result from the multi-dimensional interpolation while, beyond the range of independent variables considered, a linear extrapolation method is employed.

3.2. Control valve and other sub-models

The globe control valve has been modelled as an orifice with a variable diameter. For a given lift θ, i.e. position of the stem, the valve area ratio φ is defined as the current flow passage area divided by the maximum one. The relationship between the two parameters is reported in Eq. (7).

$$\varphi(\theta) = \frac{A(\theta)}{A(\theta = 1)} = 1.151\sqrt{\theta} - 0.151\theta$$

When the valve is fully open (θ = 1), the flow passage area is equal to the cross section of the adjacent pipes, whose inner diameter is 130 mm. To prevent any blockage of the flow, the minimum value considered for φ during the analysis is 9%. This corresponds to an equivalent diameter of the flow passage area of 39 mm and a lift θ equal to 0.63%.

The plate heat exchangers (heaters and condensers), the centrifugal pump, the receiver and the piping have been modelled using a set of dedicated templates available in the software platform and thoroughly presented in [37].

3.3. Simulation setup

The boundary conditions imposed for the system model are: the pump and expander revolution speed, the expander BIVR, the control valve area ratio, and the inlet temperatures, mass flow rates and pressures of hot and cold sources (all indicated in lowercase letters in Fig. 3). The numerical problem is solved with an implicit method that approximates the set of algebraic differential equations to a set of nonlinear algebraic ones [35].

The simulation outputs are thermal quantities since no mechanical and electrical losses have been taken into account. More specifically: the expanders power output is the twice the indicated power of each expander; the net power output is the difference between expanders and pump powers; the cycle thermal efficiency is the ratio between the net power output and the thermal power recovered at the heater (Eq. (7)).

$$\eta_{TFC} = \frac{2P_{ind} - P_{pump}}{\dot{m}_{hot}\, c_{p,hot}\, (T_{hot,in} - T_{hot,out})} \tag{7}$$

4. Results and discussion

4.1. Twin-screw expander simulations

Prior to integration of the expander model in the TFC system one, some expander-focussed simulations are presented. With reference to the boundary conditions reported in Table 2, Fig. 4 provides a comparison of the pressure and quality indicator diagrams for the BIVRs resulting from the configurations reported in Fig. 2. Fig. 5 instead summarizes the key performance parameters such as efficiency and power. Since the modelling approach herein considered does not take into account friction losses, the power reported in Fig. 5 is the indicated one, not the one at the shaft; consequently, no mechanical efficiency could be estimated.

Even if the inlet pressure was set to 5 bar, Fig. 4 shows that, regardless of the BIVR, the actual value during the suction process is always lower; this is due to the pre-expansion in the suction manifold that feeds the expander cells [36] as well as the throttling loss through the suction port, whose opening is reported in Fig. 2. Moreover, this phenomenon increases with the revolution speed. In the case of lower BIVRs, a reduction of pre-expansion is observed: for a BIVR of 5.06 the suction pressure is 4 bar, while when the BIVR is equal to 3.16 the expander cells are filled at 4.4 bar. This is consistent with findings in [22]. Beyond a BIVR of 3.16, the benefit on the pre-expansion reduction is marginal, even if the duration of the suction process is longer as one would expect from the extended positioning of the radial suction port. This phenomenon can be explained with the support of Fig. 5, which shows an increase of mass flow rate at lower BIVR for the same pressure

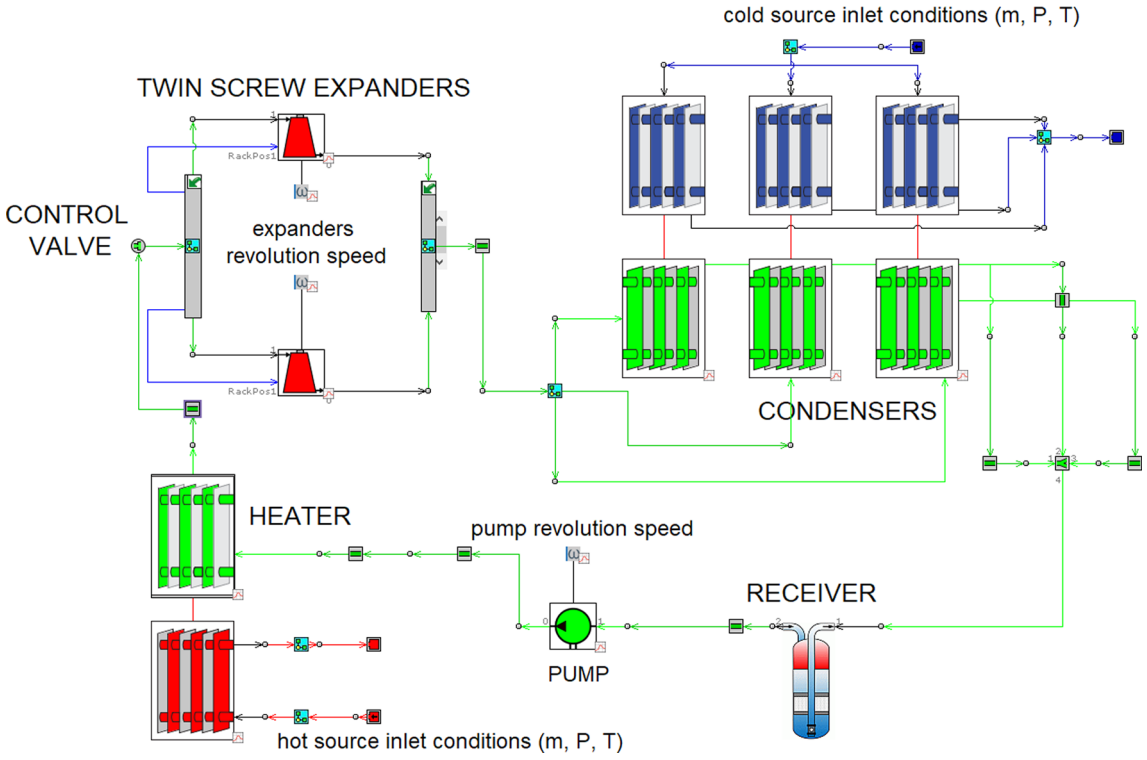

Fig. 3. TFC system model: lower case labels refer to boundary conditions.

boundary conditions of the simulations. Therefore, the larger opening due to the radial suction port allows to intake a larger amount of fluid which consequently leads the volumetric efficiency of the machine to increase. Hence, the pre-expansion decreases thanks to the increased volumetric performance. In a fixed BIVR expander operating at steady state conditions, the same benefits could be achieved through a suitable design of the intake manifold.

For the same manometric pressure ratio, lower BIVRs lead to under-expansion phenomena that can be clearly seen from Fig. 4. Moreover, one can notice that the cell pressure does not suddenly adapts to the discharge value. Similar trends have been found experimentally [25], even though the data refer to water as working fluid. This deviation from an ideal isochoric process may be due to the finite capacity of the discharge plenum as well as the gradual opening of the discharge port (Fig. 2). This aspect was also noticeable in simulations performed using the same modelling platform but with reference to a single phase ORC sliding vane expander [41]. The under-expansion leads to a decrease of the expander isentropic efficiency, as reported in Fig. 5. The total indicated power instead increases at lower BIVR due to the larger mass flow rates involved. However, due to the lower isentropic efficiency, at lower BIVRs correspond lower specific indicated powers.

4.2. TFC system simulations

To assess the impact of the main process variables on the TFC system and expander performance, a parametric study has been carried out varying the model boundary conditions with respect to the reference point presented in Table 3. For each variable changed, the remaining ones have been kept constant and equal to their reference values. The effects of these variations have been assessed from a system perspective by evaluating the cycle thermal efficiency and net power output, and from the expander one, by analysing the isentropic efficiency and the refrigerant quality at the inlet of the machine. The investigated range of the parameters varied is reported in Table 4.

4.2.1. Control valve opening

Fig. 6 shows the effects of the flow throttling through the globe valve with reference to the operating point reported in Table 3. Although the results are focussed on the valve, the simulations were carried out at system level and not considering the globe valve as a standalone component. The analysis is presented in terms of lift and area ratio, both defined in Section 3.2, and considers the pressure drop across the valve as well as the percentage variations of the volume and mass flow rates as dependent variables.

When the valve area ratio is decreased from 100% (valve fully open) to 9% (valve lift of 1%), the pressure drop increases from 0.01 bar to 3.5 bar. At the same time, the valve throttling results in a volume flow rate reduction from 100% to 15%. Since the refrigerant flashing is shifted from the heater to the control valve, the substantial decrease in the volumetric flow rate is compensated by an increase of the working fluid density at the inlet of the control valve. As such, the decrease in mass flow rate is only limited from 100% to 8%.

This phenomenon can be explained as follows: the additional pressure drop introduced by the closure of the valve undoubtedly modifies the circuit impedance. This leads the pump to supply a greater head and, in turn, a flow at higher pressure. For the same heat input at the heater, since the latent heat of vaporisation reduces at increasing pressures, the high-pressure refrigerant flow now requires a larger pre-heating compared to the reference case. As a result, at the inlet of the control valve the refrigerant flow has a higher density, because of the higher pressure, and a lower quality, due to the larger pre-heating. These operating conditions allow to balance the volume flow rate reduction.

The effects of the flow throttling via the control valve on the TFC system performance are presented in Fig. 7. From a theoretical perspective, throttling a flow upstream of an expander would have a detrimental impact on the overall power output since an expansion process across the valve does not perform any work. In the current case, however, the mass flow rate compensation discussed in Fig. 6 and the higher refrigerant quality at the inlet of the expanders instead lead to a 22% increase of the specific power output. In fact, when the valve area ratio

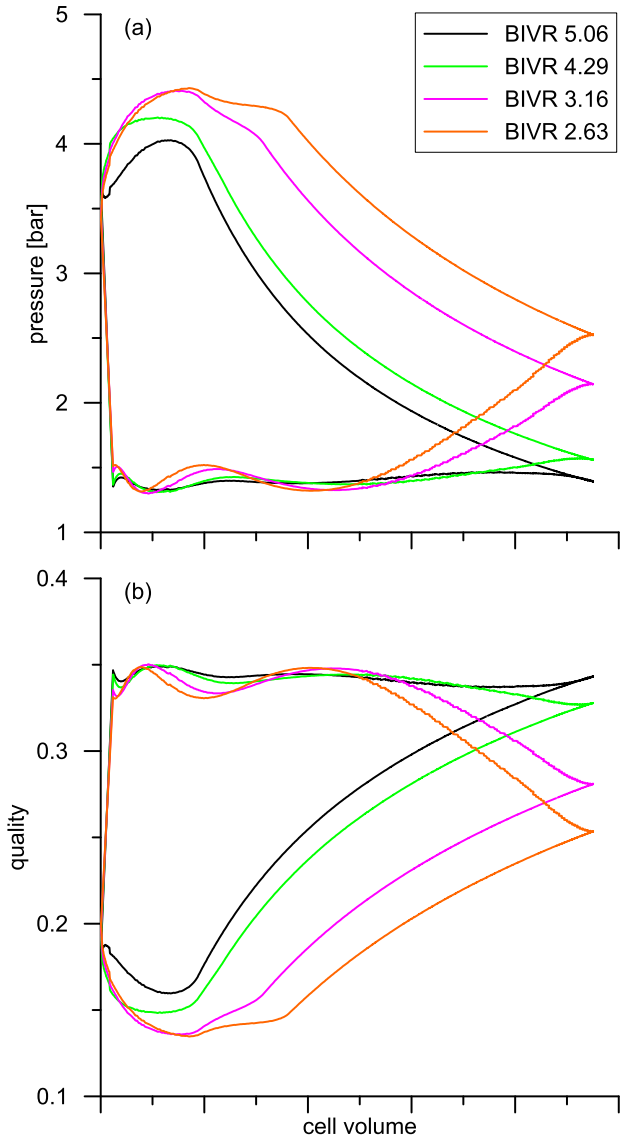

Fig. 4. Indicator pressure (a) and quality (b) diagrams at different BIVRs; simulation conditions reported in Table 2.

goes from 100% to 9%, the refrigerant quality at the inlet of the expanders increases from 0.11 to 0.16 (Fig. 7.b). For the same mass flow rate (Fig. 6), this results in an overall higher absolute enthalpy of the two-phase refrigerant flow upstream of the expanders which, in turn, generate a power output increase from 110 kW to 123 kW. With respect to the overall heat to power conversion unit, this results in a performance increase: the net power output and thermal efficiency go from 80 kW to 101 kW and from 4.3% to 5.2% respectively (Fig. 7.a).

4.2.2. Expander revolution speed

Fig. 8 shows the results obtained by varying the expander speed and maintaining constant the pump one. In particular, it is possible to observe that when the revolution speed of the expander increases from 3000 RPM to 6000 RPM, the efficiency of the machine decreases from the optimal value of 78% to the minimum of 66% (Fig. 8.b), with a consequent decrease in the power generated, from 110 kW to 90 kW. An increase of revolution speed negatively affects the filling of the machine, with a resulting drop of volumetric efficiency and power output. The reduced power generated by the expanders also leads to a decrease of the system net power output and thermal efficiency, which go from 85 kW to 61 kW and from 4.3% to 3.0% respectively (Fig. 8.a),

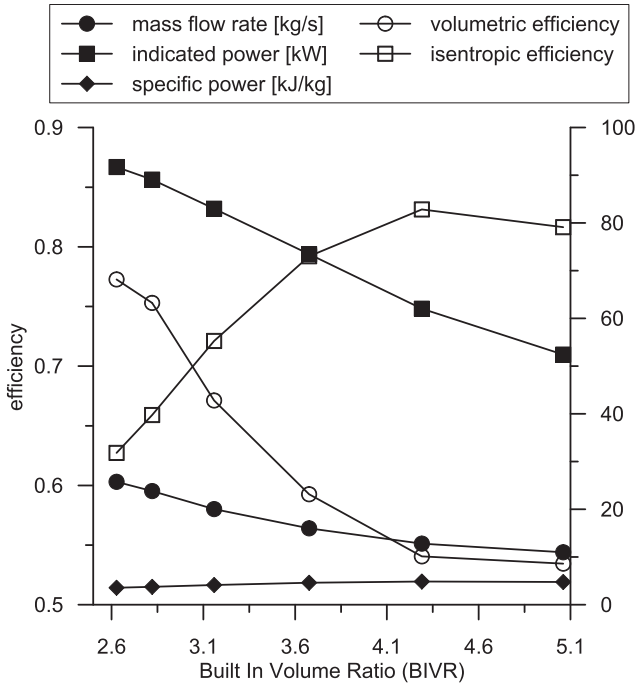

Fig. 5. Effects of BIVR on the expander performance: results refer to the same simulation conditions as in Fig. 4 (see Table 2) and are reported in terms of efficiency (left y-axis), mass flow rate, specific and absolute indicated powers (right y-axis).

Table 3
Reference operating conditions.

Cycle variables	Hot water	R245fa	Cold water
Mass flow rate [kg/s]	7.84	24.80	130.30
Inlet/Max pres [bar]	4.0	6.4	3.0
Outlet/Min pres [bar]	3.9	1.1	2.7
Inlet/Min temp [°C]	85	18	12
Outlet/Max temp [°C]	25	63	17
System performance and setup			
Net power output [kW]	81		
Thermal efficiency	4.0%		
Expander efficiency	74.0%		
Valve opening	100.0%		

Table 4
Simulation matrix for the off-design analysis of the system.

Hot source		Min	Ref	Max
Mass flow rate	kg/s	5.49	7.84	10.19
Inlet temperature	°C	75	85	95
Inlet pressure	bar	4		
Cold source				
Mass flow rate	kg/s	130.3		
Inlet temperature	°C	12		
Inlet pressure	bar	3		
TFC equipment				
Pump speed	RPM	2500	3000	3500
Expander speed	RPM	3000	4500	6000
Expander BIVR		2.63	5.06	5.06
Control valve area ratio		9.0%	67.5%	100.0%

being the pump power consumption constant (fixed pump revolution speed).

For the same expander revolution speed variation, the refrigerant quality at expander inlet increases from 0.15 to 0.20 (Fig. 8.b). In particular, higher expander speeds lead to higher volumetric flow rates processed by the machine, while the mass flow rate in the system is

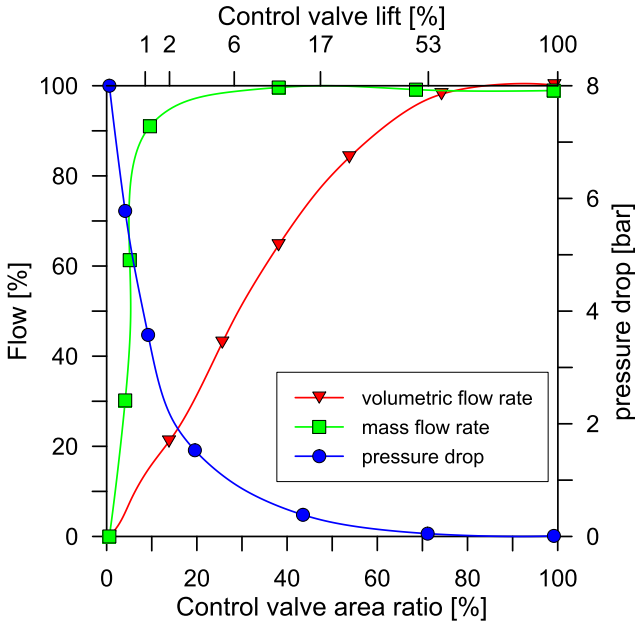

Fig. 6. Pressure drop across the globe control valve at different openings and effects on the flow rate with respect to the conditions listed in Table 3.

fixed by the constant revolution speed of the pump. Then, to balance these two quantities, the pressure at the expander inlet has to decrease, with a resulting increment of the organic fluid quality.

4.2.3. Expander built-in volume ratio

Another variable that allows further controlling of the expander operating conditions is the position of sliding valve, which affects the machine Built-In Volume Ratio (BIVR). The results of the analysis are presented in Fig. 9.

When the BIVR is increased from 2.63 (sliding valve fully open) to 5.06 (sliding valve fully closed) the pressure ratio across the machine rises from 2.2 to 3.7; as a consequence, the expander power output increases from 80 kW to 110 kW. Thus, being the pump power consumption and the thermal load at the heater fixed (pump revolution speed and inlet hot source conditions constant during this set of simulations), the TFC net power output and thermal efficiency also increase from 60 kW to 80 kW and from 3.0% to 4.5% respectively (Fig. 9.a). The lower pressure ratio achieved by lowering the expander BIVR also leads to a refrigerant quality increase at the inlet of the machine, which goes from 0.12 for a BIVR of 5.06 to 0.24 for a value of 2.63 (Fig. 9.b).

4.3. Sensitivity analysis

The impact of the operating parameters investigated in paragraph 4.2 on the TFC system performance have been compared in Fig. 10 together with the effects of pump revolution speed and heat source mass flow rate and inlet temperature. As for the methodology previously described, each variable has been individually changed from the minimum to the maximum value of their respective range (reported in Table 4), while keeping constant and equal to the reference values the remaining ones. Compared to the previous analysis, instead of considering the control valve as fully open (100% of the opening area) and the sliding valve fully tightened (BIVR of 5.1), to make a reasonable comparison, the minimum, reference and maximum values of the aforementioned variables have been set equal to 9%, 67.5%, 100% (control valve area ratio) and 2.5, 3.7, 5.1 (BIVR) respectively.

Fig. 10.a presents the analysis referred to the net power output of the TFC unit, while Fig. 10.b relates to the refrigerant quality at the expander inlet. Apart from the hot source inlet conditions, which are

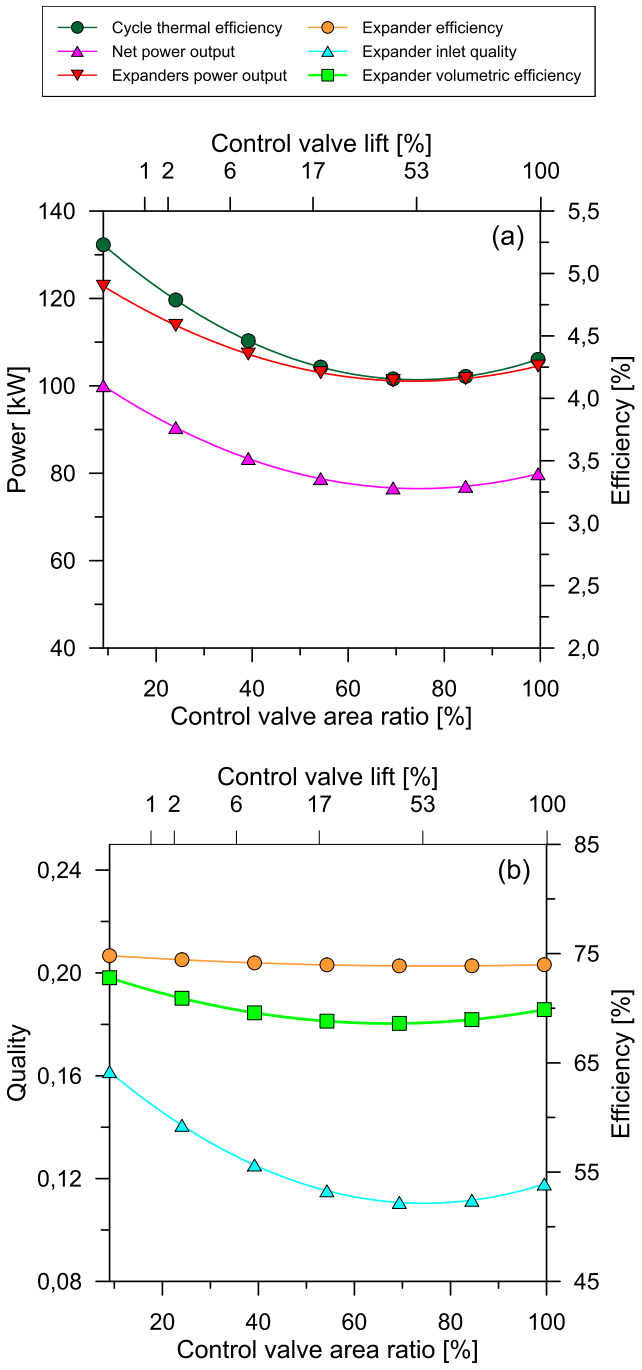

Fig. 7. Effect of the control valve area ratio on: net TFC thermal efficiency and expander power output (a), expander isentropic and volumetric efficiency as well as refrigerant quality at the expander inlet (b).

mainly related to the topping process variability, the net power output of the TFC system is particularly sensitive to a variation of the BIVR and revolution speed of the expander. The net TFC power indeed varyies from 57 kW to 83 kW and from 90 kW to 60 kW when the afore mentioned parameters span their whole ranges. The other parameters as the control valve area ratio and the pump revolution speed have a lower impact (Fig. 10a). Therefore, since the expander revolution speed and the BIVR mainly affect the efficiency of the machine and the cycle pressure ratio, these latter parameters show the most prominent impact on the system performance.

Besides the expander BIVR, the refrigerant quality at the expander inlet is strongly affected also by the pump revolution speed and the

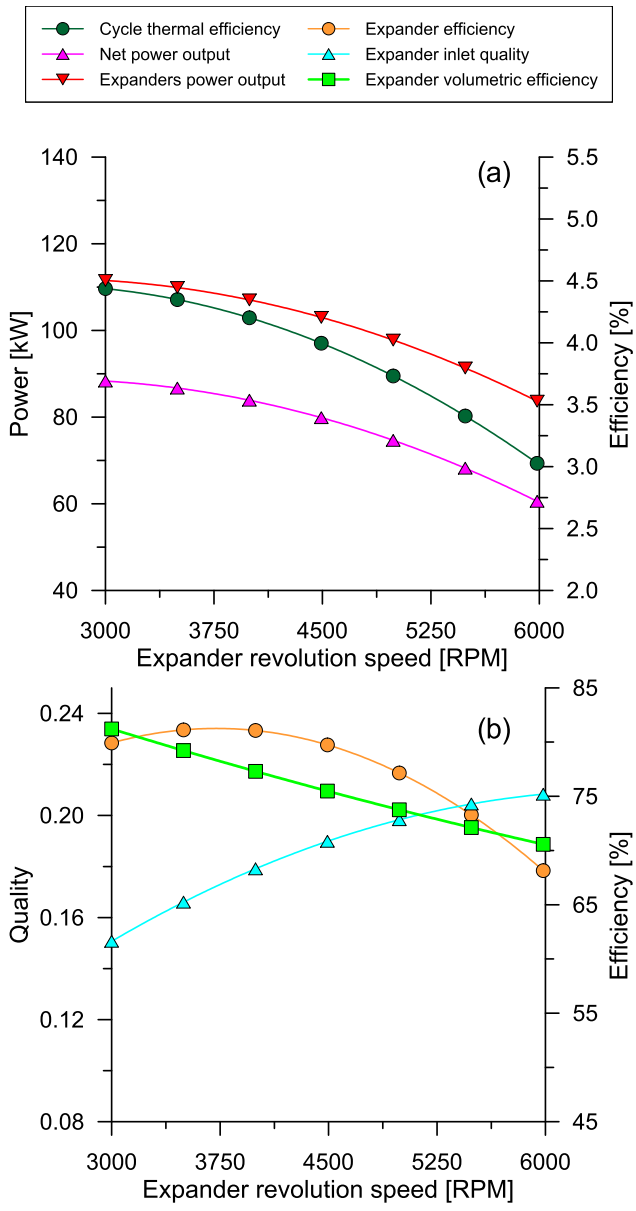

Fig. 8. Effect of the expander revolution speed on: net TFC thermal efficiency and expander power output (a), expander isentropic and volumetric efficiency as well as refrigerant quality at the expander inlet (b).

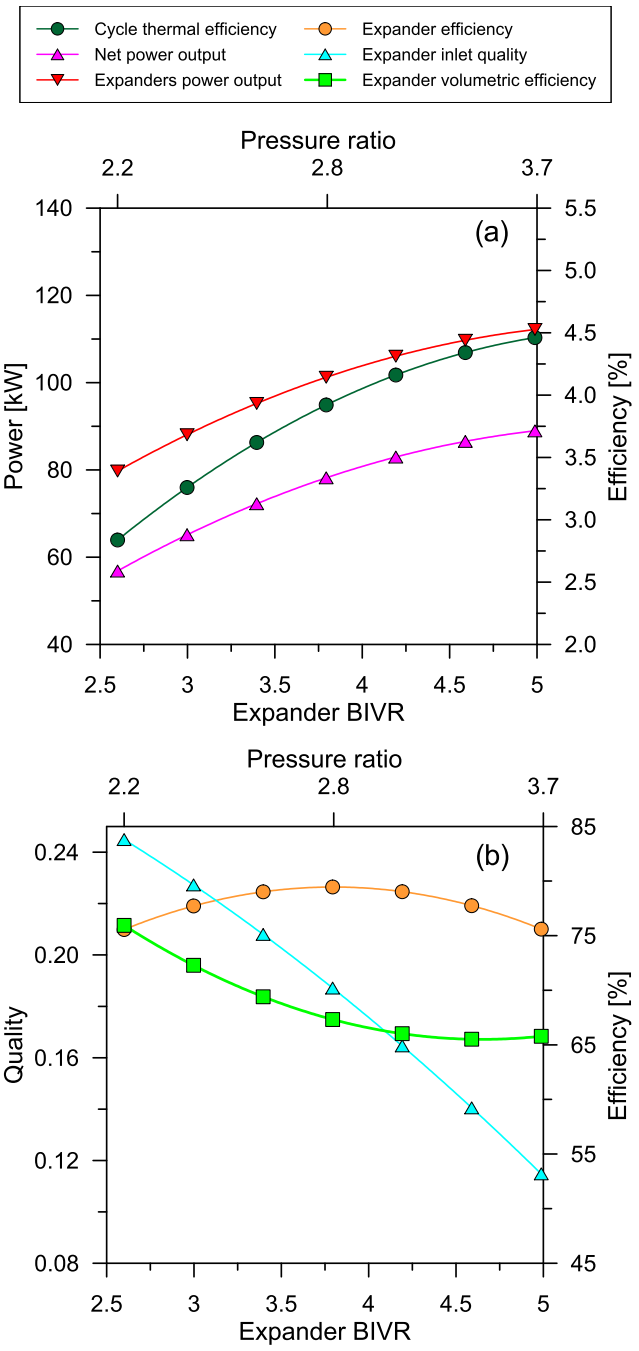

Fig. 9. Effect expander BIVR on: net TFC thermal efficiency and expander power output (a), expander isentropic and volumetric efficiency as well as refrigerant quality at the expander inlet (b).

control valve area ratio. For instance, when the pump speed is varied between its minimum and maximum values, the refrigerant quality decreases from 0.25 down to 0.18. While a decrease from 0.24 to 0.18 is observable for the same variation of the control valve area ratio. These results suggest the regulation of the expander operating conditions (i.e. revolution speed and BIVR) are of paramount importance to optimise the system performance. The pump revolution speed could be adopted as control variable to regulate the refrigerant quality at the expander inlet, which, apart from a performance perspective, it is also crucial to avoid the suction of sub-cooled liquid refrigerant at the expander inlet, which could be detrimental for the operating lifetime of the machine. Closing the control valve could be also used to regulate the vapour fraction of refrigerant, notwithstanding the dissipation introduced by its operation.

4.4. System optimisation

After the sensitivity analysis, an optimisation of the system performance has been performed for several heat source inlet conditions, i.e. inlet temperature and mass flow rate. In particular, a single objective optimisation procedure has been carried out aiming at the maximisation of the net power output. The independent variables considered were the expander BIVR and revolution speed, the pump revolution speed and the control valve area ratio. The optimisation algorithm employed was the Nelder Mead SIMPLEX one, which is a free-derivative method suitable for finding a local minimum when a not well-behaved function is considered as optimisation objective, which would make the calculation of derivatives impractical or expensive from a computational cost perspective [42].

For four independent variables as in the current case, the simplex is a pentagon and the method is a pattern search that compares function

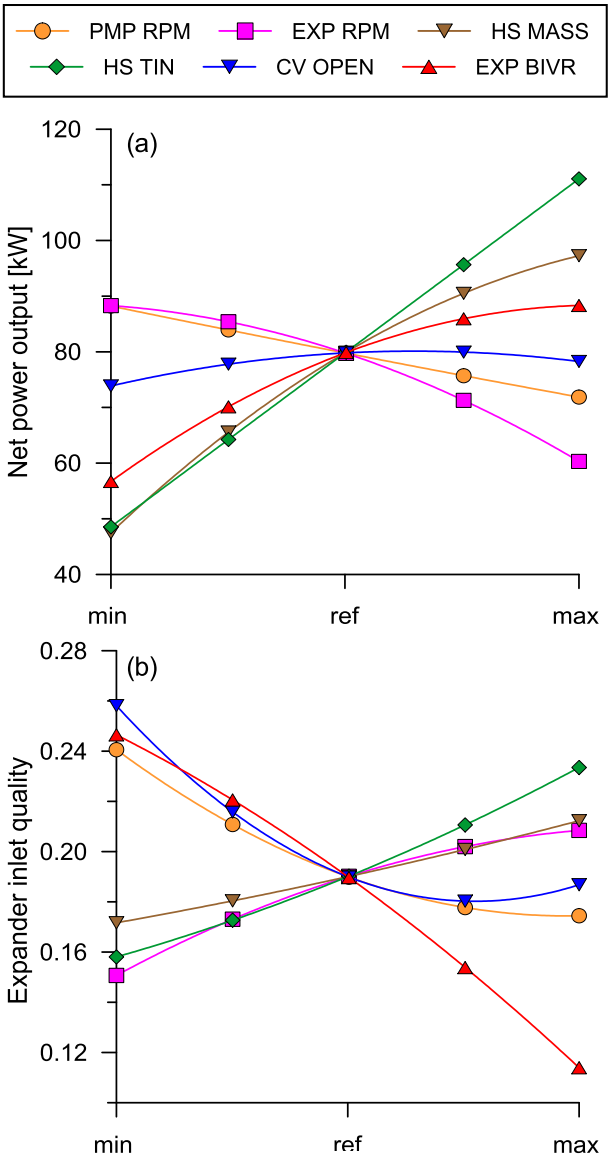

Fig. 10. Sensitivity analysis for the operating conditions listed in Table 4: net TFC power output (a), expander inlet quality (b).

values at the five vertices of the regular polygon. The worst vertex is rejected and replaced with a new one. A new pentagon is formed and the search continues. The process thus generates a sequence of pentagons for which the values of the optimization function at the vertices get smaller and smaller. The size of the polygons is reduced and the coordinates of the minimum point are found [35,42,43].

The results of the optimization procedure are shown in Fig. 11.a. It is possible to notice that the system optimisation allows to actually increase the power output achievable at reference conditions. Reducing the pump and expander speeds at 2300 RPM and 4300 RPM respectively as well as setting an expander BIVR and control valve area ratio to 3.1 and 60% respectively, the TFC unit is able to generate 103 kW instead of the 81 kW obtained in not optimised conditions. The optimisation of the main process parameters is effective when both the heat source inlet temperature and mass flow rate are varied.

At higher hot source inlet temperatures (85 °C–95 °C), when the optimised power output achieved assumes values between 85 kW and 140 kW, the optimal expander BIVR and revolution speed are in a range of 2.8–3.0 and 4500–4700 RPM respectively; the control valve is fully opened (100% of the adjacent pipe area), while the trend for pump revolution speed is not significant.

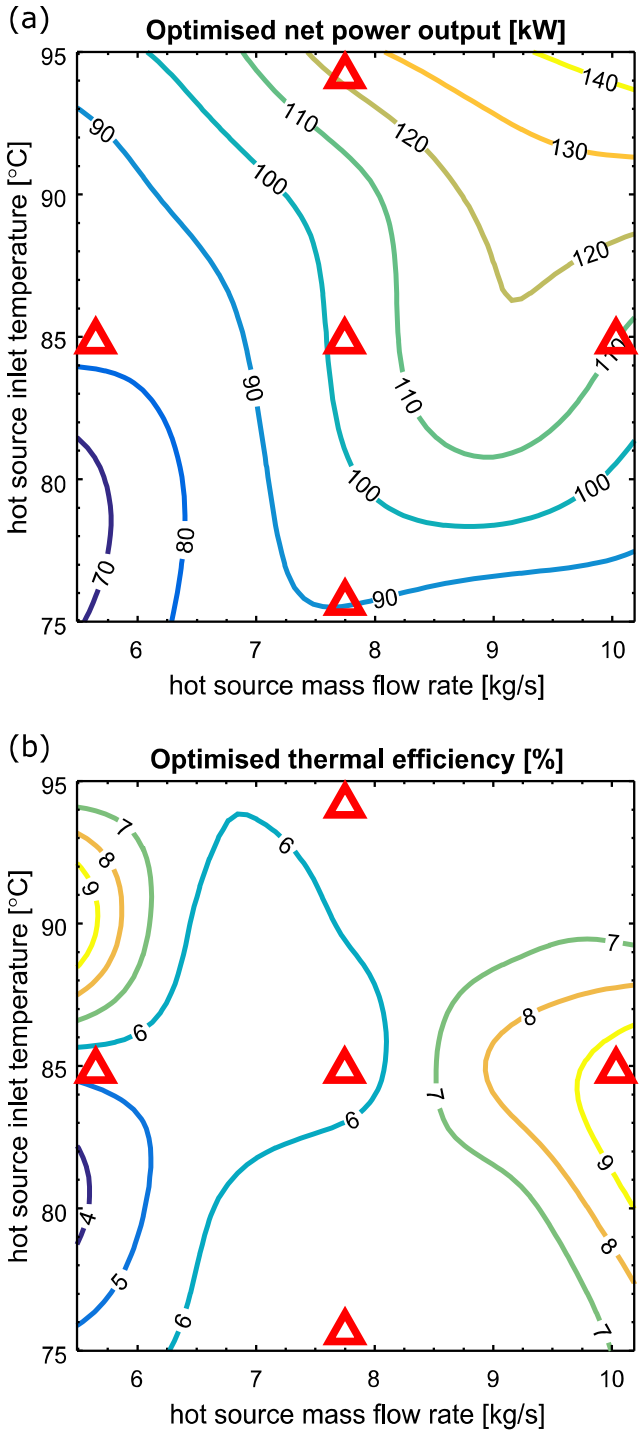

Fig. 11. Optimised performance of the TFC system: net power output (a) and thermal efficiency (b).

The lower BIVR and the full opening of the control valve lead to a higher mass flow rate of refrigerant processed by the expanders and consequently higher power generated. Furthermore, the reduced BIVR also leads to an increase of the refrigerant quality at the expander inlet; this guarantees a better machine operation. For reduced thermal loads (i.e. inlet temperature and mass flow rate of the hot source lower than 85 °C and 7.84 kg/s), on the contrary, closing the valve (27% of the adjacent pipe area) allows to generate a greater power, since it allows to balance the reduced vapour fraction due to a lower amount of thermal energy adsorbed by the fluid.

Fig. 11.b shows the system thermal efficiency achieved when the

Table 5
Optimised variables for the four cases highlighted in Fig. 11 (red triangles) and related system performance.

			Design not opt	Design opt	Case 1	Case 2	Case 3	Case 4
INPUTS	HS inlet temperature	[°C]	85	85	75	95	85	85
	HS mass flow rate	[kg/s]	7.8	7.8	7.8	7.8	5.5	10.2
OPTIMISED VARIABLES	Exp BIVR	[-]	5.06	3.5	4.7	2.9	2.5	3.0
	Exp revolution speed	[RPM]	4500	4217	2684	4477	2576	4610
	Pump revolution speed	[RPM]	3000	2448	2493	2555	2870	1635
	Control valve area ratio	[%]	100	70	61	66	40	86
OUTPUTS	Net power output	[kW]	81	103	79	124	81	122
	Thermal efficiency	[%]	4.0	6.4	6.4	6.5	5.5	9.2

unit power output is optimised. As one could expect, the lowest efficiency for the TFC unit is observable for lower thermal loads (heat source mass flow rate below 6 kg/s and inlet temperature below 85 °C), whilst at the heat source reference conditions a value of 6% is achieved. Higher efficiency values up to 9% are obtained for lower hot source mass flow rates and higher inlet temperatures (5.85 kg/s and 90 °C), and for higher hot source mass flow rates and medium inlet temperature (10.19 kg/s and 80 °C–87 °C). In these cases, the optimal system power output is achieved by lowering the pump revolution speed rather than varying other process parameters, with a consequent more beneficial effect on the unit thermal efficiency.

Table 5 provides a summary of the independent variables optimised and the corresponding TFC performance in terms of power output and thermal efficiency.

5. Conclusions

The purpose of this work was to provide insights on the operation of Trilateral Flash Cycle (TFC) systems for the conversion of low temperature (< 100 °C) waste heat sources into electricity. In a TFC system, the expansion machine can operate with different working fluids that theoretically expand from liquid saturated conditions. In the current study, a two-phase twin-screw expander with variable built-in volume ratio (BIVR) was numerically investigated as a standalone component as well as when integrated within a TFC system. The expander BIVR can be changed acting on a sliding valve on the casing of the machine that opens an additional suction port. The standalone expander simulations show that when lowering the BIVR from 5.06 to 2.63, the volumetric efficiency of the machine increases from 53% to 77%. However, the resulting under-expansion of the R245fa working fluid also leads to a drop in the isentropic efficiency from 82% to 63%, and to a reduction in the specific indicated power from 4.77 kJ/kg to 3.56 kJ/kg. On the other hand, lower BIVRs allow the expander to operate with larger mass flow rates and thus, for the same manometric pressure ratio, the total power output increases from 52.4 kW to 92.7 kW. Furthermore, the expander BIVR and revolution speed are the operating parameters that mostly affect the performance of the whole TFC system. In particular, the net TFC power output increases at higher revolution speeds and BIVRs. Besides these parameters, a lamination of the flow upstream of the expander helps to improve the power conversion even if some of the pumping power is dissipated through the valve. An optimisation study based on the Nelder-Mead Simplex algorithm enabled maximisation of the TFC power output at different mass flow rates and temperatures of the water heat source between 75 °C and 95 °C. In particular, at the hot source reference conditions (mass flow rate of 7.84 kg/s and inlet temperature of 85 °C) an optimal net power output of 103 kW and a TFC thermal efficiency of 6.4% were achieved.

Author contribution

Giuseppe Bianchi: Conceptualisation, Methodology, Software, Formal analysis, Writing, Supervision, Project administration. **Matteo Marchionni:** Methodology, Software, Formal analysis, Validation, Writing, Visualisation. **Jeremy Miller** and **Savvas A. Tassou:** Conceptualisation, Resources, Writing, Supervision, Project administration, Funding acquisition.

Declaration of Competing Interest

The authors declared that there is no conflict of interest.

Acknowledgments

Research presented in this paper has received funding from: (i) the European Union's Horizon 2020 Research and Innovation Programme under grant agreement no. 680599, (ii) Innovate UK (project no. 61995-431253, (iii) Engineering and Physical Sciences Research Council UK (EPSRC), grant no. EP/P510294/1 and (iv) Research Councils UK (RCUK), grant no. EP/K011820/1. The authors would like to acknowledge the financial support from these organizations as well as contributions from industry partners: Spirax Sarco Engineering PLC, Howden Compressors Ltd, Tata Steel, Artic Circle Ltd, Cooper Tires Ltd, Industrial Power Units Ltd. The authors also acknowledge contributions from Mr. Jonathan Harrison of Gamma Technologies during the model development. The manuscript reports all the relevant data to support understanding of the results. More detailed information and data, if required, can be obtained by contacting the corresponding author of the paper.

Appendix A. Supplementary material

Supplementary data to this article can be found online at https://doi.org/10.1016/j.applthermaleng.2020.115671.

References

[1] G. Bianchi, G.P. Panayiotou, L. Aresti, S.A. Kalogirou, G.A. Florides, K. Tsamos, S.A. Tassou, P. Christodoulides, Estimating the waste heat recovery in the European Union Industry, Energy Ecol. Environ. 4 (5) (2019) 211–221, https://doi.org/10.1007/s40974-019-00132-7.
[2] C. Forman, I.K. Muritala, R. Pardemann, B. Meyer, Estimating the global waste heat potential, Renew. Sustain. Energy Rev. 57 (2016) 1568–1579, https://doi.org/10.1016/J.RSER.2015.12.192.
[3] A. Mahmoudi, M. Fazli, M.R. Morad, A recent review of waste heat recovery by Organic Rankine Cycle, Appl. Therm. Eng. 143 (2018) 660–675, https://doi.org/10.1016/j.applthermaleng.2018.07.136.
[4] S. Iglesias Garcia, R. Ferreiro Garcia, J. Carbia Carril, D. Iglesias Garcia, A review of thermodynamic cycles used in low temperature recovery systems over the last two years, Renew. Sustain. Energy Rev. 81 (2018) 760–767, https://doi.org/10.1016/j.rser.2017.08.049.
[5] J. Fischer, Comparison of trilateral cycles and organic Rankine cycles, Energy 36 (2011) 6208–6219, https://doi.org/10.1016/j.energy.2011.07.041.
[6] N.A. Lai, J. Fischer, Efficiencies of power flash cycles, Energy 44 (2012) 1017–1027, https://doi.org/10.1016/j.energy.2012.04.046.
[7] Siemens, Steam Turbines for Geothermal Power Plants, 2013, URL: geothermal-communities.eu/assets/elearning/7.29.steam-turbines-for-geothermal-power-plants_en.pdf.
[8] Fabris, G. (2000). Two-phase reaction turbine (No. DOE/GO/10317-Q). Fas Engineering (US), URL: www.osti.gov/servlets/purl/764445.
[9] Rane, S. and He, L., 2019, August. Two-Phase Flow Analysis and Design of Geothermal Energy Turbine. In IOP Conference Series: Materials Science and Engineering (Vol. 604, No. 1, p. 012043). IOP Publishing, DOI: 10.1088/1757-

899X/604/1/012043.
[10] Elliott Group Corporation, Power Recovery Systems, 2019, URL: www.elliott-turbo.com/Files/Admin/Literature/Updated%20Cover%20092019/power%2Drecovery%2Dsystems%2Epdf.
[11] M.J. Perlmutter, H.E. Kimmel, C.H. Chiu, H. Paradowski, 2004, Economic and environmental benefits of two-phase LNG expanders, 14th Int. Conf. And exhibition on liquified natural Gas, Doha.
[12] G. Bianchi, R. McGinty, D. Oliver, D. Brightman, O. Zaher, S.A. Tassou, J. Miller, H. Jouhara, Development and analysis of a packaged Trilateral Flash Cycle system for low grade heat to power conversion applications, Thermal Sci. Eng. Progress 4 (2017) 113–121, https://doi.org/10.1016/J.TSEP.2017.09.009.
[13] M. Ahmadi, S. Vahaji, M.A. Iqbal, A. Date, A. Akbarzadeh, Experimental study of converging-diverging nozzle to generate power by Trilateral Flash Cycle (TFC), Appl. Therm. Eng. 147 (2019) 675–683, https://doi.org/10.1016/j.applthermaleng.2018.10.116.
[14] Welch, P. and Boyle, P., 2009. New turbines to enable efficient geothermal power plants. GRC Transactions, 33, pp.765-772. URL: energent.net/documents/Geothermal_Resources_Council_2009_Paper.pdf.
[15] Q. Wang, W. Wu, Z. He, D. Ziviani, Analysis of the intake process and its influence on the performance of a two-phase reciprocating expander, Appl. Thermal Eng. (2019) 113943, , https://doi.org/10.1016/j.applthermaleng.2019.113943.
[16] Öhman, H. and Lundqvist, P., 2015. Screw expanders in ORC applications, review and a new perspective. In 3rd International Seminar on ORC Power Systems, October 12-14, 2015, Brussels, Belgium.
[17] Electratherm, https://electratherm.com/products/product-brochures/.
[18] E-rational, https://www.e-rational.net/.
[19] White, M., Read, M.G. and Sayma, A.I., 2018. Using a cubic equation of state to identify optimal working fluids for an ORC operating with two-phase expansion using a twin-screw expander. URL: docs.lib.purdue.edu/iracc/1870/.
[20] I K Smith, N Stošič, C A Aldis, Development of the trilateral flash cycle system: part 3: the design of high-efficiency two-phase screw expanders, Proc. Inst. Mech. Eng. Part A: J. Power Energy 210 (1) (1996) 75–93, https://doi.org/10.1243/PIME_PROC_1996_210_010_02.
[21] M. Read, N. Stosic, I.K. Smith, Optimization of screw expanders for power recovery from low-grade heat sources, Energy Technol. Policy 1 (2014) 131–142, https://doi.org/10.1080/23317000.2014.969454.
[22] Vasuthevan, H and Brümmer, A., 2016, Thermodynamic Modeling of Screw Expander in a Trilateral Flash Cycle. International Compressor Engineering Conference. Paper 2475. URL: https://docs.lib.purdue.edu/icec/2475.
[23] A. Nikolov, A. Brümmer, Impact of different clearance heights on the operation of a water-flooded twin-screw expander—experimental investigations based on indicator diagrams, IOP Conf. Ser.: Mater. Sci. Eng. 425 (2018) 12008, https://doi.org/10.1088/1757-899X/425/1/012008.
[24] B. Sångfors, Effect of Steam Quality X upon the Water/Steam Flow Consumption as a function of generated effect (2015), https://doi.org/10.13140/RG.2.1.3795.1444.
[25] Nikolov, A., Brümmer, A., 2016. Analysis of Indicator Diagrams of a Water Injected Twin-shaft Screw-type Expander. International Compressor Engineering Conference. Paper 2492. URL: https://docs.lib.purdue.edu/icec/2492.
[26] H. Öhman, Low temperature difference power systems and implications of multi-phase screw expanders in Organic Rankine Cycles (Doctoral dissertation, KTH Royal Institute of Technology), 2016.
[27] McKay, R., 1982. Helical screw expander evaluation project final report DOE/ET/28329-1.
[28] R.F.J. Steidel, H. Weiss, J.E. Flower, Performance Characteristics of the Lysholm Engine as Tested for Geothermal Power Applications in the Imperial Valley, J. Eng. Power 104 (1982) 231–240.
[29] Grieb, M. and Brümmer, A., 2019, August. Investigation into the effects of surface condensation in steam-driven twin screw expanders. In IOP Conference Series: Mater. Sci. Eng. (Vol. 604, No. 1, p. 012044). IOP Publishing. DOI:10.1088/1757-899X/604/1/012044.
[30] S. Lecompte, M. van den Broek, M. De Paepe, Design of an optical-access expansion chamber for two-phase expansion, Proceedings of ECOS 2017 – The 30th Environmental Conference on Efficiency, Cost, Optimization, Simulation and Environmental Impact of Energy Systems, 2017.
[31] H. Kanno, N. Shikazono, Modeling study on two-phase adiabatic expansion in a reciprocating expander, Int. J. Heat Mass Transf. 104 (2017) 142–148, https://doi.org/10.1016/J.IJHEATMASSTRANSFER.2016.07.106.
[32] B.J. Woodland, D. Ziviani, J.E. Braun, E.A. Groll, Considerations on alternative organic Rankine Cycle configurations for low-grade waste heat recovery, Energy 193 (2020), https://doi.org/10.1016/j.energy.2019.116810.
[33] M. Yari, A.S. Mehr, V. Zare, S.M.S. Mahmoudi, M.A. Rosen, Exergoeconomic comparison of TLC (trilateral Rankine cycle), ORC (organic Rankine cycle) and Kalina cycle using a low grade heat source, Energy 83 (2015) 712–722, https://doi.org/10.1016/j.energy.2015.02.080.
[34] Yaodong Zhou, Fengyuan Zhang, Lijun Yu, Performance analysis of the partial evaporating organic Rankine cycle (PEORC) using zeotropic mixtures, Energy Convers. Manage. 129 (2016) 89–99, https://doi.org/10.1016/j.enconman.2016.10.009.
[35] Gamma Technologies, GT-SUITE-Flow, Theory Manual (2019).
[36] G. Bianchi, S. Kennedy, O. Zaher, S.A. Tassou, J. Miller, H. Jouhara, Numerical modeling of a two-phase twin-screw expander for Trilateral Flash Cycle applications, Int. J. Refrig. 88 (2018) 248–259, https://doi.org/10.1016/J.IJREFRIG.2018.02.001.
[37] M. Marchionni, G. Bianchi, A. Karvountzis-Kontakiotis, A. Pesyridis, S.A. Tassou, An appraisal of proportional integral control strategies for small scale waste heat to power conversion units based on Organic Rankine Cycles, Energy 163 (2018) 1062–1076, https://doi.org/10.1016/J.ENERGY.2018.08.156.
[38] PDManalysis, Screw Compressor Rotor Grid Generator SCORG, URL: pdmanalysis.co.uk/scorg/.
[39] Y. Qi, Y. Yu, Thermodynamic simulation on the performance of twin screw expander applied in geothermal power generation, Energies (2016), https://doi.org/10.3390/en9090694.
[40] E.W. Lemmon, M.L. Huber, M.O. Mclinden, NIST Reference Fluid Thermodynamic and Transport Properties—, REFPROP User's Guide, 2013.
[41] Fabio Fatigati, Giuseppe Bianchi, Roberto Cipollone, Development and numerical modelling of a supercharging technique for positive displacement expanders, Appl. Therm. Eng. 140 (2018) 208–216, https://doi.org/10.1016/j.applthermaleng.2018.05.046.
[42] J.A. Nelder, R. Mead, A Simplex Method for Function Minimization, Comput. J. 7 (1965) 308–313, https://doi.org/10.1093/comjnl/7.4.308.
[43] J.C. Lagarias, J.A. Reeds, M.H. Wright, P.E. Wright, Convergence properties of the nelder-mead simplex method in low dimensions, SIAM J. Optim. 9 (1998) 112–147, https://doi.org/10.1137/S1052623496303470.